LA-UR--91-1490

DE91 013651

TITLE SYNTHESIS OF METASTABLE ALUMINUM-BASED INTERMETALLICS BY MECHANICAL ALLOYING

AUTHOR(S)
R. B. Schwarz
S. Srinivasan
P. Desch

SUBMITTED TO International Symposium on Mechnical Alloying, Kyoto, Japan, May 7-10, 1991. Proceedings to be published in Materials Science Forum, Trans Tech Publications

DISCLAIMER

Los Alamos National Laboratory
Los Alamos, New Mexico 87545

Paper of talk presented at the International Symposium on Mechanical Alloying, Kyoto, Japan, May 7-10. 1991. Proceeding to be published in *Materials Science Forum*, Trans Tech Publications.

SYNTHESIS OF METASTABLE ALUMINUM-BASED INTERMETALLICS BY MECHANICAL ALLOYING

R. B. Schwarz, S. Srinivasan, and P. B. Desch

Center for Materials Science
Los Alamos National Laboratory
Los Alamos, NM 87545

ABSTRACT

We have used mechanical alloying (MA) to prepare fine-grained powders of Al 25 at.% X (X = Ti, Zr, Hf) having the metastable cubic $L1_2$ structure. Hexane (C_6H_{14}) is added to the milling media to avoid the agglomeration of the aluminum powder. Carbon from the decomposition of the hexane incorporates into the powder to form a fine dispersion of carbides. These carbides are beneficial because they limit grain growth during consolidation and add strength to the alloy.

We have consolidated the mechanically alloyed powders using conventional hot-pressing and non-conventional dynamic pressing. We used hot pressing to consolidate mechanically alloyed $L1_2$-Al_3Ti powder in the presence of excess of Al. The compact has the DO_{22} structure. Its room-temperature compressive strength is 1.2 GPa (exceeding that of cast Al_3Ti by a factor of 10). At 400°C, the compressive strength decreases to 1 GPa. The ductility, which is negligible at room temperature, increases to 6% at 400°C. We used dynamic pressing to consolidate $L1_2$-Al_5CuZr_2 powder. The compact, having the $L1_2$ structure, has fine grains (44 nm) and a fine dispersion of ZrC precipitates (7 nm). Its hardness is in the range of 1030 kg mm^{-2}. Current efforts are to investigate ternary alloys based on fine-grained trialuminides which include a ductile second phase.

1. INTRODUCTION

In terms of properties, ordered intermetallics occupy an intermediate position between solution- and precipitation-strengthened metallic alloys on the one extreme, and ceramics on the other. The most attractive property of ordered intermetallic compounds is their strength, which is maintained at elevated temperatures. Some of these compounds, especially those having the $L1_2$ structure, show an increasing yield strength with increasing temperature. Other desirable characteristics of intermetallics are low self-diffusion rates and high elastic moduli, which are also maintained at high temperatures. Ordered compounds of the form

Al_3X (X = transition metal) can have very low densities. The low density combined with the high strength and modulus give rise to very attractive specific properties (property divided by density). Ordered intermetallic compounds, however, are generally brittle for temperatures below a few hundred centigrade and this severely limits their use.

Most of the research on ordered intermetallics is now directed at understanding the lack of low-temperature ductility. This characteristic has been attributed to intrinsic factors such as low crystal symmetry (e.g. alloys with tetragonal DO_{22} and DO_{23} structure), low cleavage strength, and extrinsic factors like grain boundary structure, segregation of impurities to grain boundaries, and environmental factors affecting primarily the grain boundaries [1].

In this paper we address trialuminides and related compounds. In equilibrium, most binary trialuminides have the tetragonal DO_{23} or DO_{22} structures, Fig. 1, which are closely related to the cubic $L1_2$ structure. The DO_{23} structure can be derived from the $L1_2$ by displacing every second (001) plane by a vector (½,½,0). Similarly, the DO_{22} structure can be derived from the $L1_2$ by displacing every (001) plane by the same vector. Experience has shown that the number of slip systems that are activated in the DO_{23} and DO_{22} systems before fracture occurs is less than five, the minimum number required by the von Mises criterion for compatibility in the plastic deformation of polycrystals [2,3]. Consequently, considerable effort is being made to develop pseudo-binary alloys which have the $L1_2$ structure, under the assumption that enough equivalent slip systems would result in increased ductility. So far, the results of these studies have not been encouraging. The "crystal structure control" approach has had some success, with a limited number of $L1_2$-structure intermetallics showing some ductility, but many exhibiting almost no ductile behavior [4,5].

The lack of ductility in $L1_2$ materials is attributed to the high anti-phase boundary (APB) energy on both (111) and (100) planes. For example, Fu [6] calculates APB energies for Al_3Sc, which is stable in the $L1_2$ structure, of 670 and 450 mJ m^2 for the (111) and (100) planes, respectively. Such high APB energies (approximately a factor of 3 higher than in ductile Ni_3Al) mean that superdislocations having Burgers vector $\mathbf{b} = <110>$ are only slightly dissociated on either plane [7]. Thus, during slip, the total superdislocation has to be nucleated essentially at the same time [6], a process that may require a local stress that exceeds the cleavage stress. Recent theoretical calculations [8] indicate that the APB energy in (metastable) $L1_2$-Al_3Ti is due to a strong hybridization between Ti-*d* and Al-*p* orbitals. This interaction seems to also determine the relative stability of the phases in which Al_3X alloys form. For example, Hong et al. [8] claim that Al_3Ti crystallizes in the DO_{22} structure, rather than in the $L1_2$ structure, because the DO_{22} structure has more Ti-Al second-nearest-neighbor bonds than $L1_2$. From these theoretical studies it follows that simple concepts such as atomic size and electronegativity are not sufficient to give even a qualitative picture of the relative phase stability of ordered intermetallic compounds; electronic bonding and how it is affected by alloying must be considered in detail.

The present work is aimed at understanding the synthesis and properties of binary and pseudo-binary alloys based on the formula Al_3X, where X is a transition metal. We have used mechanical alloying (MA), a high-energy ball milling technique, to prepare alloy powders which we consolidate by conventional (hot pressing) and dynamic techniques. MA has various

advantages over conventional processing techniques such as arc casting. These include: (a) mechanically alloyed powders have highly homogeneous compositions; (b) MA usually yields metastable phases which enables us to measure the relative stabilities between phases; (c) MA enables properties modification by the introduction of a fine, homogeneous dispersions of precipitates such as carbides; and (d) mechanically alloyed powders usually have extremely small grain size, with little or no solute segregation to grain boundaries or surfaces. Reduction in grain size is another technique which may lead to increased ductility [9].

2. METHODS

The starting materials were commercial powders of at least 99.99% purity, with the exception of the zirconium powder which was 99.9% pure. The MA was done in SPEX 8000 laboratory-size mills. We used vials and milling media made either of tungsten carbide or hardened steel. When using a tungsten carbide vial, which cannot be effectively sealed, the milling was done inside a glove box (oxygen and water content less than 1 ppm). When using steel vials, the milling was done in air, with the vial and lid sealed with an elastomer O-ring. Hexane (C_6H_{14}) was then used as a surfactant to prevent agglomeration of the aluminum powder on the walls of the container and on the balls during MA. Following the milling, the hexane was removed by evaporation in vacuum. The addition and removal of the hexane was done in a well ventilated fume hood because of the toxicity of hexane vapors. Typically, for 20 h of MA, between 0.05 and 0.15 g of hexane is retained in the 5 g powder charge. In previous work [10], we determined that the hexane decomposes into elemental carbon and hydrogen which go into solution. The hydrogen can be removed by annealing the powder in vacuum. The carbon combines with the transition metal forming carbides.

With MA there is always the danger that erosion of the container and/or balls may introduce impurities into the alloyed powder. Using hexane as a surfactant, it is relatively easy to clean the vial and balls at the end of each milling process. The constancy of the weight of the vial and balls after a large number of milling operation indicates that this contamination, if present, is less than 0.01 wt%.

We used two powder-consolidation techniques. Al-12.5 at.% Cu-25 at.% Zr powder (henceforth denoted Al-12.5Cu-25Zr) having the $L1_2$ structure was consolidated by a dynamic method. The powder was encapsulated into a stainless steel tube which was evacuated while being heated. Upon reaching a temperature of 900°C and a pressure below 10 mtorr, the tube was pressed in a Ram press while maintaining the vacuum. Al_3Ti powder was consolidated by pressing at 830°C in a graphite die. The die was heated by eddy currents in an argon atmosphere. Upon reaching the compaction temperature of 830°C, the pressure was increased to 1800 psi and maintained for 15 min. The die was then furnace cooled. Before pressing, the Al_3Ti powder was degassed in vacuum at 400°C for 1 h.

The structures of the powders and compacts were determined by x-ray diffraction using Mo-K_α radiation. The powders were also studied by differential scanning calorimetry (DSC) to measure reaction enthalpies and transformation temperatures. These tests were done at the heating rate of 20 K min^{-1}, using a continuous flow of high-purity argon at 40 cc min^{-1}.

3. RESULTS

3.1 Evolution of the MA Process

Figure 2 shows the change in the lattice parameter of aluminum as a function of MA time during the synthesis of $L1_2$-Al_3Zr. The figure includes data for steel milling media (50 hardened steel balls, 1/4" diameter) and tungsten carbide media (1 ball, 7/16" diam.), with the vials made of the same material as the balls. Hexane was added to the steel milling media. For both milling media, the change in lattice parameter with MA shows two distinct regimes. Initially, $\Delta a/a$ increases with increasing MA time, reaching a saturation value of $\Delta a/a = 1.2\%$. Notice that the same saturation value is obtained for MA with and without hexane. The processing time at which $\Delta a/a$ reaches saturation coincides with the first appearance of $L1_2$ superlattice lines on the x-ray diffraction patterns. This time is indicated by the dashed line for the powders milled in steel media. For the powders milled with WC media, the superlattice reflections were absent at 20 h of MA, but were clearly visible at 68 h of MA. These observations suggest that the large lattice parameter increase is due to the dissolution of zirconium in aluminum. Notice further that once the Al(Zr) solid solution starts ordering into the $L1_2$ structure, the lattice dilation ceases although more Zr is being incorporated into the alloy.

To estimate the amount of zirconium that triggers the fcc→ $L1_2$ transformation we need to know the partial gram-atomic volume of zirconium in aluminum, v_{Zr}. In the absence of this value (Zr has a very limited solubility in Al at room temperature), we followed the suggestion of Turnbull [11]; he notices that for Al-Fe and Al-Mn alloys, v_{TM} is approximately the same in the solid solution as in the intermetallic compounds richest in aluminum. He suggests that this result may also apply to other Al-transition metal alloys. Using data for Al_3Zr (the intermetallic richest in aluminum) we deduced $v_{Zr} = 12.0$ cm^3 g-at^{-1}, which is larger than $v^o_{Al} = 10.0$ cm^3 g-at^{-1}, but significantly smaller than $v^o_{Zr} = 14.1$ cm^3 g-at^{-1}. With these values we deduce that the fcc→ $L1_2$ transformation occurs when aluminum contains, on the average, approximately 16.5 at% Zr in solution. This value, however, could be off by as much as a factor of two because of the uncertainty in our estimate of v_{Zr}.

3.2 Carbide Formation During MA with Hexane

As stated before, the MA of aluminum-rich alloys at room temperature requires the use of a surfactant. The high-energy attrition during MA causes some of the surfactant to incorporate into the powder [10]. It is apparent that this is not a purely mechanical process (i.e., entrapment of hexane) but involves a chemical reaction. Table 1 gives the amount of hexane retained in the powder during the synthesis of Al_3Zr starting from Al + Zr and from Al + ZrH_2. That the amount of hexane pick up is significantly greater when using elemental Zr than when using ZrH_2 suggesting that Zr acts as a catalyst for the decomposition of the hexane, a process that must precede its absorption into the Al_3Zr lattice. The hydrogen is removed by vacuum annealing in the temperature range 300-450 °C. The carbon combines with Zr to form fine carbides. When starting from mixtures of Al + Zr powders, ZrC forms

during the milling process, whereas when starting from Al + ZrH_2, the carbide forms during the subsequent anneal.

The volume fraction of carbide has an influence on the thermal stability of the $L1_2$ phase. Figure 3 shows DSC curves for Al_3Zr powder prepared from Al + ZrH_2 (curve A) and Al + Zr (curve B) powder mixtures. The carbide content in these alloys is given in Table 1. We can see that the increase in carbide content raises the $L1_2 \rightarrow DO_{23}$ transformation temperature by approximately 50 K. We cannot ascertain if this temperature shift is an intrinsic effect of the carbides (e.g., carbides becoming obstacles to shear on (001) planes, which is necessary for the transformation) or the effect of the shift in the overall alloy composition caused by the removal of Zr which forms carbide.

Table 1. Amount of hexane pick up and weight percent carbon incorporated in the MA powders. Powder charge of 5 g.

Starting powder	Hexane pick up	C wt% calculated	C wt% measured(1)	Phases detected in as-milled powder
Al + Zr	0.21 g	3.39	2.51	$Al_3Zr(L1_2)$ + ZrC
Al + ZrH_2	0.04 g	0.66	1.18	$Al_3Zr(L1_2)$ + ZrH_2

(1) combustion chemical analysis using a Leco carbon/sulfur analyzer

3.3 Thermal Stabilities of the Trialuminides.

In the as-mechanically alloyed condition, Al_3X (X = Ti, Zr, Hf) have the (metastable) $L1_2$ structure. During annealing, these alloys transform into more stable phases. Figure 4 shows the transformation temperatures of Al_3X powders prepared from mixtures of elemental powders. We have found [12] that before Al_3Ti transforms to the stable DO_{22} phase, it transforms to a second metastable DO_{23} phase. The $L1_2 \rightarrow DO_{23}$ transformation temperatures increase in going from Ti to Zr to Hf. We have no clear explanation for this trend. The changes in transformation temperature could reflect differences in the atomic volumes of the transition elements since these should correlate with their chemical diffusivity in the alloy [13]. However, this model does not explain the data because Hf has a smaller atomic volume than Zr. We have also calculated the partial molar volumes of Ti, Zr, and Hf in aluminum using the approximate method suggested by Turnbull [11]. We obtain 8.4, 12, and 10.8 cm^3 g-at, respectively, again showing that Hf has a smaller volume than Zr. A more plausible explanation for the increase in thermal stability of the $L1_2$-Al_3X phase in going from X = Ti to Zr to Hf can be given in terms of the total energy difference, $\Delta E(L1_2 - DO_{23})$, between the $L1_2$ and DO_{23} phases. The electronic structure calculations of Carlsson and Meschter [14] predict that $\Delta E(L1_2 - DO_{23})$ decreases in going from Ti to Zr to Hf, so that the driving force for the transformation decreases in that order.

We have investigated ternary additions of various transition metals (Li, Mg, Cr, Fe, Ni, Cu) to mechanically alloyed Al_3X (X = Ti, Zr, Hf) as a means of increasing the stability of the $L1_2$ structure [13,15]. The highest stability is obtained with copper; Al-12.5Cu-25Zr and Al-12.5Cu-25Ti are stable in the $L1_2$ structure to at least 1300°C.

3.4 Consolidation of Mechanically Alloyed Al-12.5Cu-25Zr Powder

Although the mechanically alloyed Al-12.5Cu-25Zr and Al-12.5Cu-25Ti powders are stable with respect to structural transformation to at least 1300°C, they are metastable with respect to grain growth. Avoiding grain growth during consolidation suggests the use of non-conventional powder sintering techniques such as dynamic compaction [16]. We used a modified dynamic vacuum hot-forging technique (see section 2) to consolidate Al-12.5Cu-25Zr powder [15,17]. This powder was prepared by mechanically alloying the proper amounts of Al, Cu, and ZrH_2 in the presence of hexane. From Table 1 we deduce that this powder had about 1.2 wt% C. The compacts had the $L1_2$ structure and were fully dense. Indentation tests were performed with a Vickers diamond pyramidal hardness indenter using 50 and 200 g loads. The lack of material squeezed out at the edges of the indent, and the fine cracks seen at some of the vertices of the indent suggest that the material has very limited ductility. The hardness deduced from the size of these indents (neglecting possible cracking) is 1033 kg mm^{-2}. These values are about a factor of 3 higher than the hardness of 360 kg mm^{-2} measured by Virk and Varin [18] in induction-melted samples. This difference may be due to the carbide dispersion in our alloys. The samples prepared by the dynamic hot forging technique were too small for performing other mechanical tests.

Transmission electron microscopy (TEM) specimens were prepared by mechanical polishing, followed by ion thinning [19]. Figure 5 shows a bright field transmission TEM of compacted Al-12.5Cu-25Zr. The $L1_2$ grains have a very uniform size distribution of approximately 44 nm. A few large grains (several μm in size) were sometimes detected suggesting that the consolidation temperature of 900°C may have been too high. In addition to the $L1_2$ grains, the TEM micrograph shows a uniform distribution of small dots. Through higher magnification TEM and selected area diffraction we identified these dots as cubic ZrC precipitates, 7 nm in size [19]. These small and stable precipitates are most likely beneficial to the thermal stability and strength of the alloy, especially at high temperatures since they help limit grain growth during the consolidation of the powders [20,21].

3.5 Consolidation of Mechanically Alloyed Al_3Ti Powder

We consolidated Al_3Ti using conventional hot pressing [12]. Powder with the average composition $Al_{80}Ti_{20}$ was prepared by mechanically alloying the proper amounts of Al and Ti for 20 h in the presence of hexane. 0.11 g of hexane was retained in the powder. Assuming that all the carbon combined with Ti to form TiC, we estimate that the powder had about 1.8 wt% C. This corresponds approximately 9 wt% TiC in the final alloy. The compact, 3.2 cm in diameter and 0.6 cm in thickness, had a density of 3.25 g cm^{-3} and an estimated porosity below 4%. The starting powder had excess Al, most of which was squeezed out of the die during consolidation. We determined that 10.6 wt% (12 vol%) Al remained in the compact

by measuring its heat of fusion in the calorimeter. Thus, the "Al_3Ti" compact is in reality a three-phase alloy of Al_3Ti - 11 wt% Al - 9 wt% TiC.

Figure 6 is a SEM micrograph of an etched surface of the "Al_3Ti" compact. The selective etching of Al reveals Al_3Ti regions separated by narrow channels of Al. The Al_3Ti regions are approximately 1 to 3 μm in size. Figure 7 is a TEM micrograph of the "Al_3Ti" compact. Three adjacent grains, two of Al_3Ti and one of Al, have been brought into diffraction condition by tilting the sample. The grains are approximately 0.5 μm in size. Cubic TiC precipitates are superposed on the Al_3Ti grains. A detailed analysis of various micrographs shows that the TiC precipitates have plate morphology, approximately 30 nm in diameter, and reside at the grain boundaries. No TiC precipitates are seen on the Al grains. Because the Al-12.5Cu-25Zr and Al_3Ti powders had similar initial grain sizes, it is clear from Figs. 5 and 7 that the longer time at high-temperature during conventional hot pressing contributes significantly to grain growth in the aluminide. The TEM micrographs reveal that the Al grains are connected to other Al grains, forming an extended network, as also suggested by the SEM micrograph of Fig. 6. The Al_3Ti regions within the Al network are made up of many grains.

Cylindrical samples, 0.5 cm diameter and 0.6 cm long, were cut from the compact by spark machining. These samples were deformed in compression at a strain rate of $2x10^{-4}$ s^{-1} at temperatures between 300 and 773 K [22]. Figure 8 shows temperature depe ıdences of the yield stress (determined from the intersection of tangents drawn to the elastic and the initial plastic portions of the stress-strain curves), and the plastic strain to fracture. SEM observation of fracture surfaces show that the "Al_3Ti" deformed at room temperature failed by a combination of intergranular and transgranular fracture. At the test temperature of 773 K the samples were highly ductile, enabling deformations of more than 80%. Also shown in the figure are the compression test results of Yamaguchi et al. [2] for vacuum-induction melted polycrystalline Al_3Ti having an average grain size of 1 mm. We observe that the mechanically alloyed "Al_3Ti" has a compressive yield strength approximately an order of magnitude higher than that of conventionally-prepared large-grain single-phase Al_3Ti. The higher strength is most likely due to the TiC precipitates. The strain to fracture follows a similar trend, being significantly higher for the MA samples. We attribute this difference to the presence of Al (second phase) and to the finer grain size. The abrupt decrease in the strength beyond 650 K is due to the presence of Al.

4. DISCUSSION

Synthesizing intermetallic alloys by MA has several advantages over conventional casting. Some of these are: (a) the possibility of synthesizing metastable phases such as $L1_2$ structure Al_3Ti, Al_3Zr and Al_3Hf; (b) grain refinement to nanocrystalline levels (9 nm in as mechanically alloyed Al-12.5Cu-25Zr [15]); and (c) the possibility of introducing a homogeneous dispersion of fine precipitates (7 nm in consolidated Al-12.5Cu-25Zr [19]). We have seen in this work that the volume fraction of carbide precipitates can be controlled by milling mixtures of Al + X, or Al + XH_2 (X = Ti, Zr, Hf) and that the temperature and time of consolidation determine the final grain size of the compacts.

Comparison of the strength and ductility of the "Al_3Ti" alloy prepared by MA and the Al_3Ti alloy prepared by conventional casting [2] (Fig. 8) clearly demonstrates the salutary effects of the fine grain and carbide precipitates in the former. The carbide precipitates may also contribute to the increased high-temperature strength in the "$AlTi_3$" compact (400 MPa versus 105 MPa at 800K), in spite of the presence of low-melting aluminum in the "Al_3Ti" sample. The compositional homogeneity of the MA processed material may also be a factor contributing to the improvement in properties.

Although the present improvement in strength is encouraging, the room temperature ductility is clearly insufficient. Factors such as reduced grain size, a more symmetric structure ($L1_2$ in Al-12.5Cu-25Zr), and ductile second phase (Al in "Al_3Ti") do not seem to improve the room temperature ductility. As a whole, except for Ni_3Al, recent research in intermetallics (NiAl [23], and TiAl [24]) has led to only moderate improvements in low-temperature ductility. Studies of the electronic structure of intermetallics have been enlightening in terms of identifying the factors responsible for low-temperature brittle behavior [6,8,14,25,26] but a solution to the problem appears distant. Most intermetallics are intrinsically brittle, a consequence of their ordered structure. Ironically, the ordering is also responsible for the high-temperature strength and stiffness of these alloys. Theoretical considerations suggest ductility in intermetallics could be enhanced by ternary additions which would (a) decrease the twin energy [23] and (b) decrease the ordering and thus the APB energies [6]. Most likely, achieving these goals would result in a lower strength. Another possibility which should be explored is partially ordered intermetallics. Stoloff and Davies [7] have shown that disordering the lattices of Cu_3Au and Ni_3Mn, and other intermetallics, facilitates the generation and glide of unit dislocations, rather than superdislocations. This results in an increased ductility and, surprisingly, in an increase in strength because of work hardening.

ACKNOWLEDGEMENTS

We thank S. R. Chen for help in the compression tests. The work by P. B. Desch is in partial fulfillment of the requirements for a Ph.D. degree at IIT. This work was supported by the U.S. Department of Energy, Office of Basic Energy Sciences and by Laboratory Directed Research and Development funds.

REFERENCES

1. Liu, C. T.: in *Alloy Phase Stability*, Eds. G. M. Stocks and A. Gonis, Kluwer Academic Publ., (1989), p.7.
2. Yamaguchi, M., Umakoshi, Y., and Yamane, T.: *Phil. Mag.*, 1987, 55, 301.
3. Umakoshi, Y., Yamaguchi, M., Yamane, T., and Hirano, T.: *Phil. Mag.*, 1988, 58, 651.
4. Izumi, O., and Takasugi, T.: *J. Mater. Res.*, 1988, 3, 426.
5. George, E.P., Horton, J.A., Porter, W.D., and Schneibel, J.H.: *J. Mater. Res.*, 1990, 5, 1639.
6. Fu, C.L.: *J. Mater. Res.*, 1990, 5, 971.
7. Stoloff, N.S., Davies, R.G.: *Acta Metall.*, 1964, 12, 473.

8. Hong, T., Watson-Yang, T.J., Freeman, A.J., Oguchi, T., Jian-Hua Xu: *Phys. Rev. B*, 1990, 41, 12462.
9. Schulson, E.M., and Barker, D.R., *Scripta Met.*, 1983, 17, 519.
10. Schwarz, R.B., Hannigan, J.W, Sheinberg, H., and Tiainen, T.: *Modern Devel. Powder. Metall.*, 1988, 21, 415.
11. Turnbull, D.: *Acta Metall.*, 1990, 38, 243.
12. Srinivasan, S., and Schwarz, R.B.: unpublished results, 1991.
13. Schwarz, R.B., Desch, P.B., Srinivasan, S, and Nash, P.: in "Proc. Acta Metall. Conf. on Materials with Ultrafine Microstructures", Atlantic City, NJ., October 1990. *Acta Metall.*, 1991, in press.
14. Carlsson, A.E. and Meschter, P. J.: *J. Mater. Res.*, 1989, 4, 1060.
15. Desch, P.B.,Schwarz, R. B.:, Nash, P.: *J. Less Common Metals*, 1991, 168, 69.
16. Schwarz, R.B.. Kasiraj, P., Vreeland, Jr., T., and Ahrens, T.J.: *Acta Metall.*, 1984, 32, 1235.
17. Desch, P.B, Schwarz, R.B., and Nash. P.:, *Mater. Res. Soc. Symp. Proc*, in press (1990).
18. Virk, I.S. and Varin, R.A.: *Scripta Metall.*, 1991, 25, 85.
19. Mitchell, T.E., Desch, P.B., and Schwarz, R. B.: Proc. XIIth Intl. Cong. Electr. Microsc., San Francisco Press, San Francisco, (1990). p. 970.
20. Copley, S.M. and Kear, B.H.:, *Trans. AIME*, 1967, 239, 984.
21. Schwarz, R.B. and Nash, P.: *J. Metals,* 1989, 41(1), 27.
22. Srinivasan, S., Chen, S.R., and Schwarz, R.B.: unpublished results, 1991.
23. Darolia, R.: *J. of Metals*, 1991, 43, 44.
24. Kawabata, T., Tadano, M., and Izumi, O.: *Scripta Metall.* 1988, 22, 1725.
25. Nicholson, D.M., Stocks, G.M., Temmerman, W.M., Sterne, P., and Pettifor, D.G.: *Mater. Res. Soc. Symp. Proc.*, 1989, 133, 17.
26. Takasugi, T., Izumi, O., Masahashi, N.: *Acta Metall.*, 1985, 33, 1259.

FIGURE CAPTIONS

FIG. 1 Schematic of ordered crystal structures for A_3B - type alloys.

FIG. 2 Change in the lattice parameter of aluminum in mechanically alloyed Al_3Zr as a function of mechanical alloying time.

FIG. 3 Differential scanning calorimetry plots for Al_3Zr prepared (A) from Al + ZrH_2 and (B) from Al + Zr. The second peak, with onset at 660^oC, is from Al melting in the reference cup of the calorimeter. This peak is used for calibration.

FIG 4. Thermal stabilities of mechanically alloyed Al_3X (X = Ti, Zr, Hf). The melting temperatures of the compounds are shown at the right of the figure.

FIG 5 Transmission electron micrograph of consolidated Al_5CuZr_2. The label on the micrograph is 310 nm long.

FIG. 6 SEM micrograph of consolidated "Al_3Ti", etched to reveal Al inclusions.

FIG. 7 Transmission electron micrograph of consolidated "Al_3Ti". The label on the micrograph is 310 nm long.

FIG. 8 Compressive yield stress (open circles) and strain to failure (open triangles) of "Al_3Ti" as a function of temperature. The closed symbols are corresponding data for large-grain single-phase Al_3Ti from ref. 2.

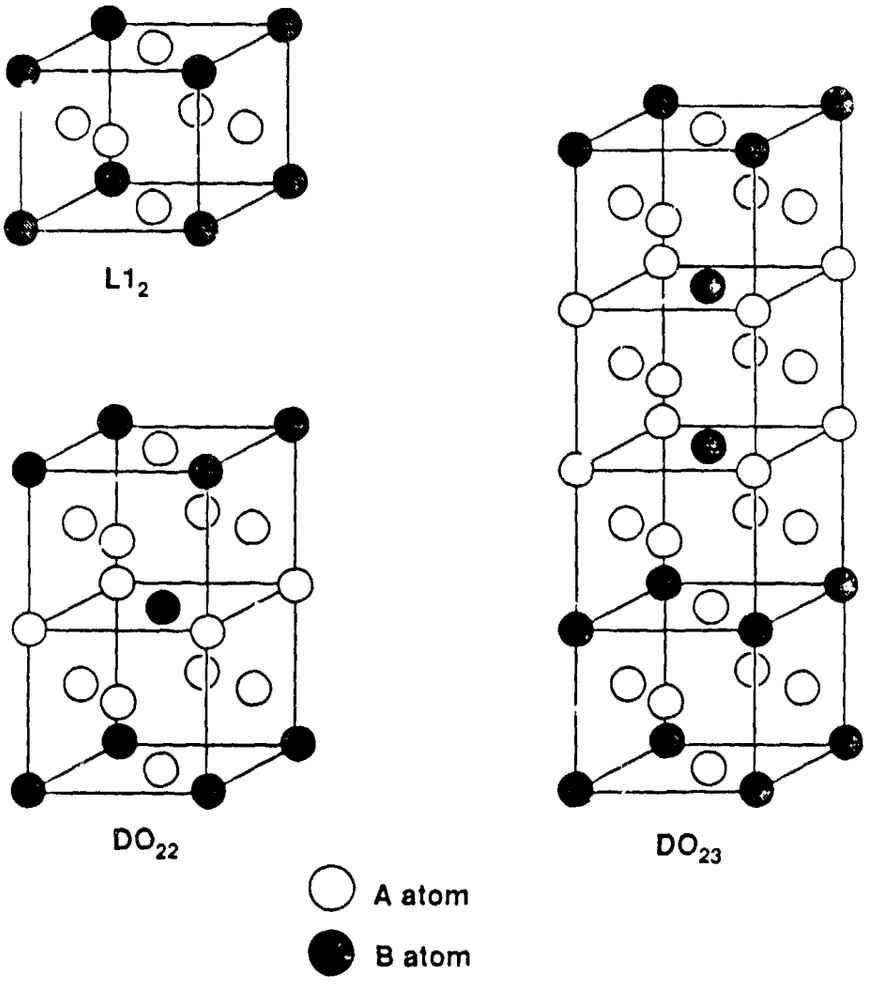

A_3B Type Structures

Fig. 1

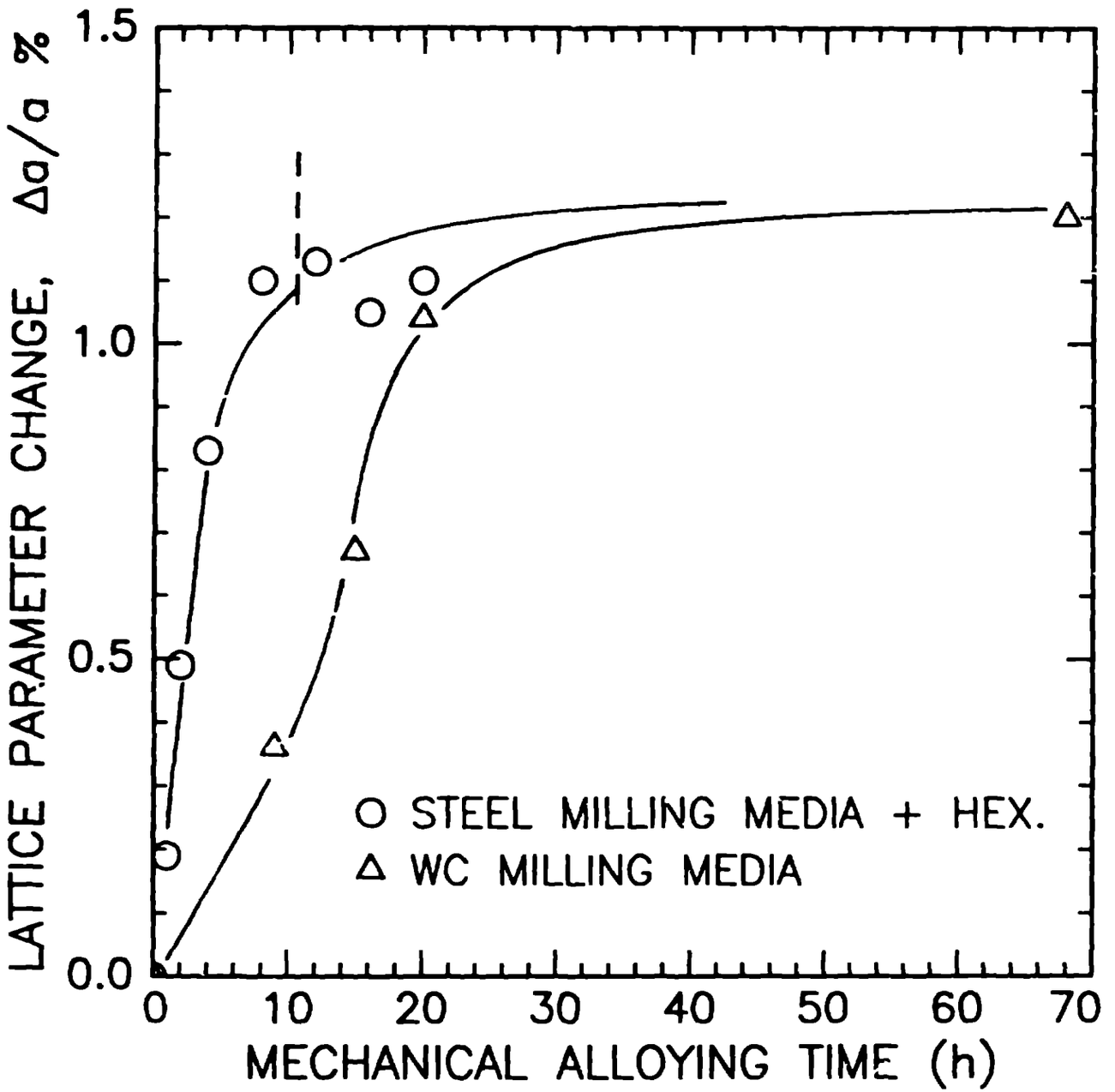
LATTICE PARAMETER CHANGE, Δa/a %
1.5
1.0
0.5
0.0
0
10
20
30
40
50
60
70
MECHANICAL ALLOYING TIME (h)
O STEEL MILLING MEDIA + HEX.
Δ WC MILLING MEDIA

Fig 2

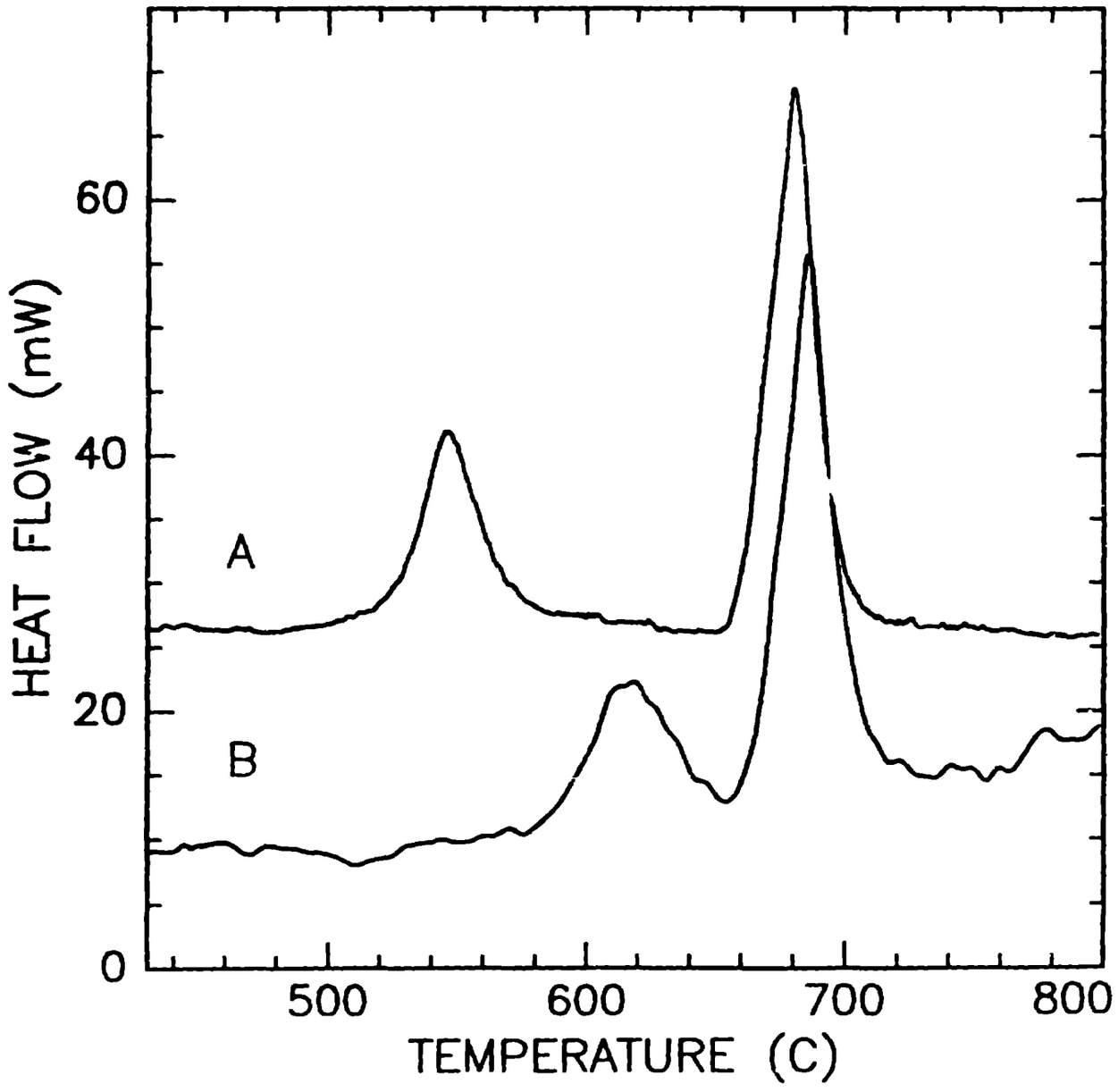

Fig 3

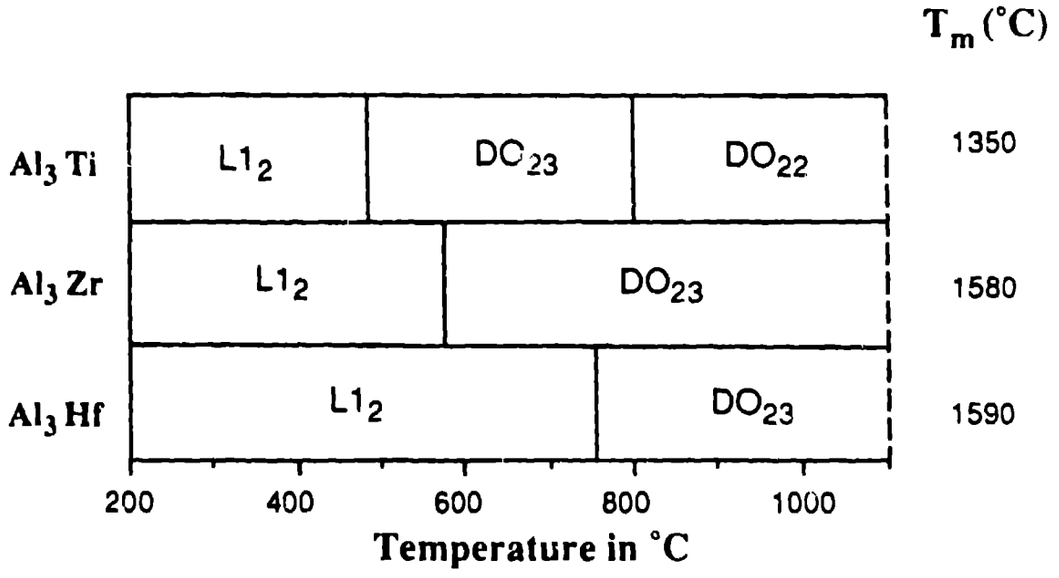
T_m (°C)
Al_3Ti
$L1_2$
DO_{23}
DO_{22}
1350
Al_3Zr
$L1_2$
DO_{23}
1580
Al_3Hf
$L1_2$
DO_{23}
1590
200
400
600
800
1000
Temperature in °C

Fig. 4

Fig. 5

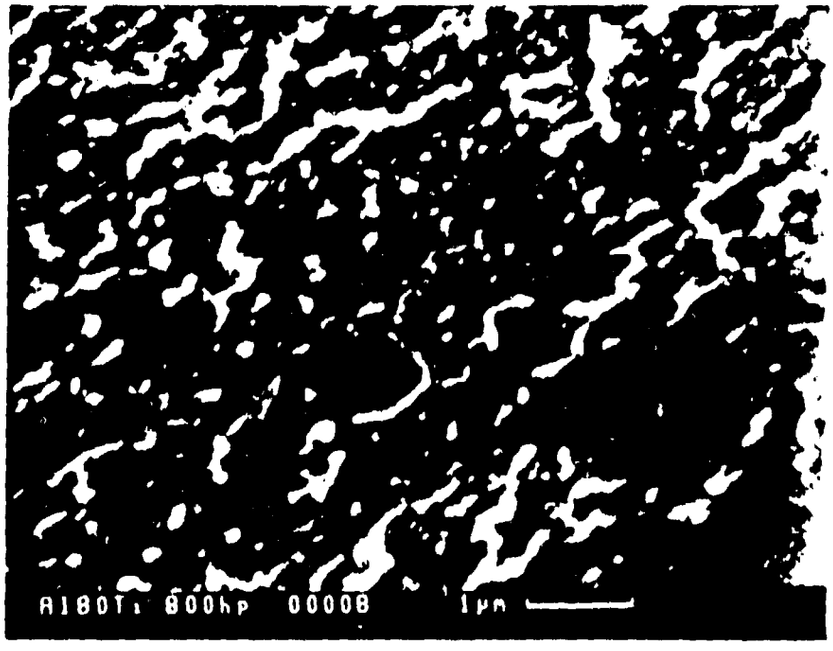

Fig. 6

Fig. 7

Fig. 5

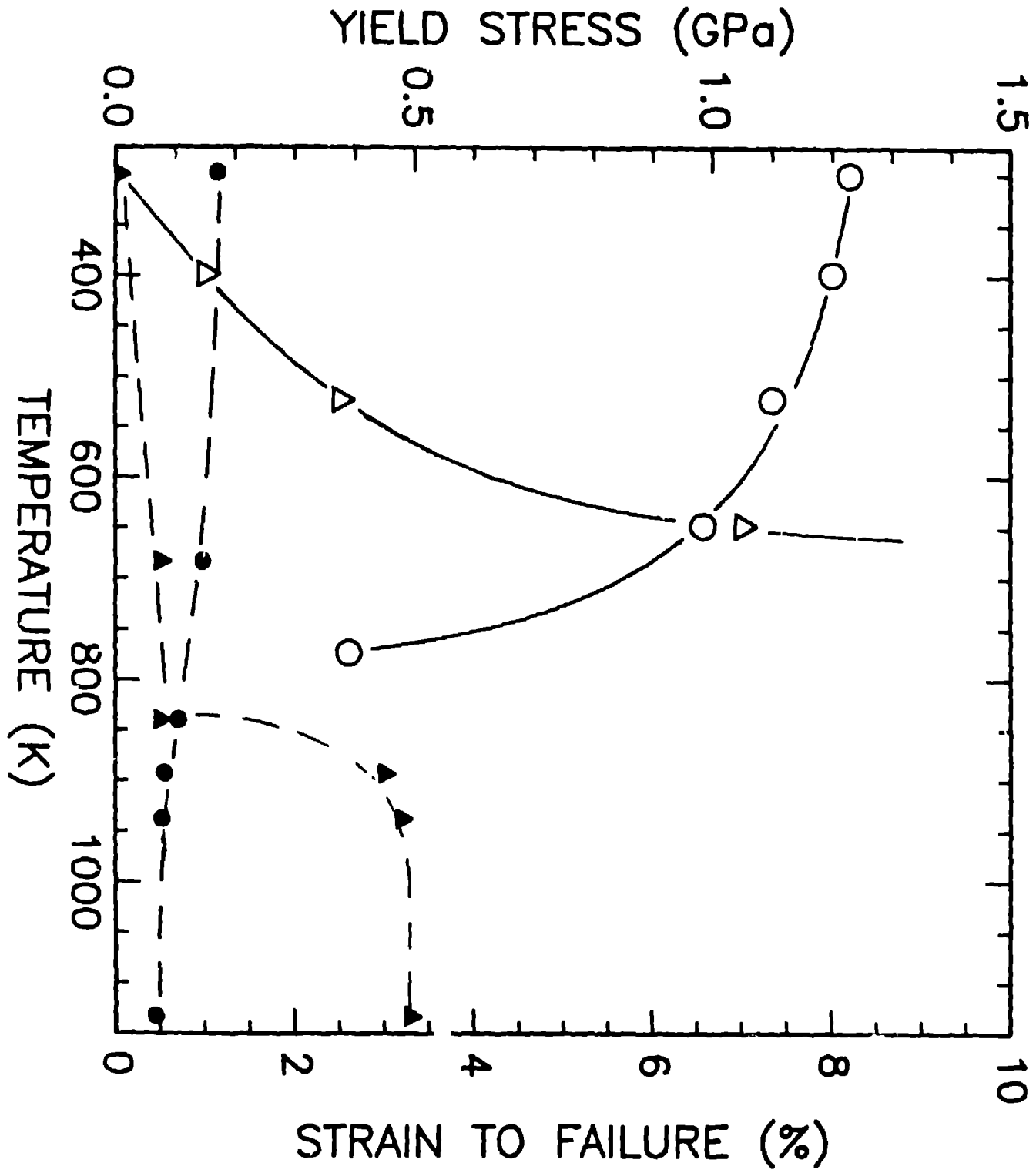
YIELD STRESS (GPa)
0.0
0.5
1.0
1.5
TEMPERATURE (K)
400
600
800
1000
0
2
4
6
8
10
STRAIN TO FAILURE (%)